Angewandte Chemie
Eine Zeitschrift der Gesellschaft Deutscher Chemiker

Supporting Information

Coloration in Supraparticles Assembled from Polyhedral Metal-Organic Framework Particles

J. Wang, Y. Liu, G. Bleyer, E. S. A. Goerlitzer, S. Englisch, T. Przybilla, C. F. Mbah, M. Engel, E. Spiecker, I. Imaz, D. Maspoch*, N. Vogel**

Experimental Procedures

Materials. Zirconium (IV) chloride ($ZrCl_4$), cetyltrimethylammonium bromide (CTAB), terephthalic acid (1,4-BDC), oxalylchloride, tetrahydrofurane, trimethylamine, O,O-bis(2-aminopropyl) polypropylene glycol-block-polyethylene glycol-*block*-polypropylene glycol 900 (Jeffamine D-900) and polyvinylpyrrolidone (Mw 10000) were purchased from Sigma Aldrich. Glacial acetic acid and *N*,*N*-dimethylformamide (DMF) were purchased from Fisher Chemical. 2-methylimidazole (2-MiM), zinc acetate dihydrate ($Zn(CH_3COO)_2{\cdot}2H_2O$) and zinc nitrate hexahydrate ($Zn(NO_3)_2{\cdot}6H_2O$) were purchased from TCI Chemical. Krytox 157 FSH and HFE 7100 were purchased from Dupont and 3M company, respectively. Lutensol (TO 8) was kindly provided by BASF. All chemical reagents and solvents were used as received without further purification. De-ionized (DI) water was obtained from a Milli-Q water purification system.

Characterization. Field-emission Scanning Electron Microscopy images were collected on SEM FEI Magellan 400L XHR at an acceleration voltage of 2.0 kV and on a Zeiss Gemini 500 SEM with the SE2 detector and an acceleration voltage of 1kV. The average size distribution of each synthesized MOF particle was statistically estimated from FESEM images by counting the sizes of 200 particles at different areas from each sample. X-ray Powder diffraction (PXRD) diagrams were collected on a Panalytical X'pert diffractometer with monochromatic Cu-Ka radiation (lCu = 1.5406 A). Zeta potential (ζ) was measured using a Malvern Zetasizer (Malvern Instruments, UK).

Synthesis of cubic C-ZIF-8 particles. In a typical synthesis, $Zn(NO_3)_2{\cdot}6H_2O$ (140 mg) dissolved in 8 mL of water was added to 24 mL of an aqueous solution containing 2-MiM (1920 mg) and 4 mL of 0.85 mg mL^{-1} CTAB solution. After standing for 5 h, the resulting ZIF-8 particles were washed with deionized water (10 mL) upon centrifugation at 9000 rpm in 50-mL Falcon tubes. The zeta potential of the resulting cubic ZIF-8 particles was approximately +30 mV.

Synthesis of truncated rhombic dodecahedral TRD-ZIF-8 particles with truncation *t* = 0.68. TRD-ZIF-8 particles were produced by following the protocol reported in a previous work. [1] Typically, $Zn(CH_3COO)_2{\cdot}2H_2O$ (300 mg) dissolved in 5 mL of water was added to 5 mL of an aqueous solution containing 2-MiM (2.72 M) and CTAB (0.54 mM) with gentle stirring. The mixture was left at room temperature for 2 h, and the resulting TRD-ZIF-8 particles with a size of 181 ± 9 nm were washed with deionized water (10 mL) upon centrifugation at 9000 rpm in 50-mL Falcon tubes. The zeta potential of the resulting TRD-ZIF-8 particles was approximately +30 mV. The conditions used for the synthesis of the other TRD ZIF-8 particles were as follows: for 198 ± 10 nm, [2-MiM] = 2.58 M and [CTAB] = 0.54 mM; for 229 ± 9 nm, [2-MiM] = 2.72 M and [CTAB] = 0.44 mM; and for 247 ± 10 nm, [2-MiM] = 2.72 M and [CTAB] = 0.54 mM.

SUPPORTING INFORMATION

Synthesis of rhombic dodecahedral RD-ZIF-8 particles. An aqueous solution (5 mL) of $Zn(CH_3COO)_2 \cdot 2H_2O$ (334 mg) was added to 5 mL of an aqueous solution of 2-MiM (1.30 g) with gentle stirring. Then, the mixture was left at room temperature for 2 h. The resulting RD-ZIF-8 particles with a size of 293 ± 13 nm were washed with deionized water (10 mL) upon centrifugation at 9000 rpm in 50-mL Falcon tubes. The zeta potential of the resulting RD ZIF-8 particles was approximately + 30 mV. The conditions used for the synthesis of the other RD ZIF-8 particles were as follows: for 246 ± 12 nm, the mass of 2-MiM was 1.34 g; and for 267 ± 12 nm, the mass of 2-MiM was 1.32 g.

Synthesis of octahedral O-UiO-66 particles. O-UiO-66 particles were produced by following the protocol reported in a previous work.[1] Typically, $ZrCl_4$ (34.9 mg) and 1,4-BDC (24.9 mg) were dissolved in 10 mL of DMF containing 2.1 M acetic acid and transferred to a scintillation vial. This mixture was heated at 120 °C for 12 h. Afterwards, the synthesized particles with an edge size of 238 ± 13 nm were washed twice with DMF (10 mL) and twice with methanol (10 mL) upon centrifugation at 9000 rpm in 50-mL Falcon tubes. The zeta potential of the resulting octahedral UiO-66 particles was approximately +45 mV. The conditions used for the synthesis of the other O-UiO-66 particles were as follows: for 194 ± 12 nm, the $ZrCl_4$ was dried in the oven for 2 hours; and for 247 ± 13 nm, a concentration of 2.45 M of acetic acid was used.

Synthesis of the perfluorosurfactant.

The synthesis protocol followed the literature.[2,3] In short, 10 g of Krytox 157 FSH was dissolved in 30 mL of HFE 7100. The solution was placed in ice bath. 2.1 mL of oxalylchloride was injected into the solution, followed by a drop of DMF. The mixture was stirred for 2 h until no gas development. After evaporation of the solution, the reaction mixture was redissolved in 30 mL of HFE 7100 oil. 1.6 g of Jeffamine D-900 was dissolved in 30 mL of anhydrous tetrahydrofurane, followed by 1.7 mL of triethylamine. The HFE 7100 solution was then injected into the THF solution while stirring overnight in open atmosphere. At inert conditions, the reaction yielded Krytox-PEG surfactant. In open atmosphere, the reaction yielded Krytox-ammonium salt. After synthesis, the reaction mixture was evaporated, leaving whitish honey-like viscous fluid, which was purified by dissolution in a mixture of HFE 7100 and methanol. The mixture was centrifuged at 11000 rpm for 20 min, ant the supernatant was removed. The purification step was repeated four times. The remaining fluid was vacuum dried to obtain the pure surfactant.

Assembly of MOF supraparticles.

Initially, 0.5 wt% non-ionic alcohol ethoxylate surfactant (Lutensol TO-8, BASF) and polyvinylpyrrolidone were added into separate dispersions of the ZIF-8 and O-UiO-66 particles, respectively, to improve their colloidal stability. This was followed by three centrifuge cycles to remove residual reagents, including any excess surfactant. Next, each aqueous MOF particle dispersion was emulsified in perfluorinated oil (HFE 7500), either by vigorous shaking or by droplet-based microfluidics.

For the first case, water-in-oil droplets were obtained by pipetting 10 µL of MOF aqueous colloid dispersion into 200 µL HFE 7500 oil (containing 1 wt% perfluorosurfactant) directly in a 1.5 mL glass vial. After sealing the vial with a cap, the vial was shaken vigorously by hand. After emulsification, the cap was removed to allow droplet

evaporation at room temperature overnight. After droplet drying, the consolidated MOF supraparticles were suspended in the remaining oil phase. With ~40 mg/mL MOF particle concentration, this procedure produces 2 mg /mL supraparticle concentration in HFE 7500 oil. Note that such supraparticles can exhibit a broad size distribution with supraparticle sizes between ~10 µm and ~50 µm, caused by the inhomogeneous droplet formation process. Nevertheless, this method is valuable as a simple procedure to screen for formation efficiencies of supraparticles, provide sufficient material for macroscopic characterization and to produce polydisperse sample to study the influence of supraparticle size on the reflected color intensity.

For the supraparticles synthesized through droplet-based microfluidics, the MOF colloidal particle dispersion and the perfluorinated oil HFE 7500 (containing 1 wt% perfluorosurfactant) were pumped into PDMS microfluidic through HDPE tube at 50 µL/hr and 300 µL/hr rate. Droplets were collected by inserting 1 mL pipette tip at the microfluidic outlet and subsequently transferred to 1.5 mL glass vial for storage and drying at room temperature overnight. After droplet drying, the consolidated MOF supraparticles were suspended in the remaining oil phase. Supraparticles formed by droplet-based microfluidics exhibited superior uniformity, with relative polydispersity below 5%. The size of the resultant supraparticles can be adjusted by changing the flow rates, the concentration of the colloidal dispersions, and the channel widths of the chip. These variations allow fabrication of uniform supraparticles between approximately 10 µm and 50 µm. Samples produced by microfluidics were used for the detailed investigation of the optical properties of individual supraparticles.

X-ray image of MOF supraparticles.

A droplet of MOF supraparticle suspension was casted on a TEM grid. The grid containing the dried MOF supraparticles was mounted on a sample holder clip and inserted into the X-ray microscope (Zeiss Xradia 810 Ultra, 5,4 keV X-rays). The MOF supraparticles were imaged in high resolution Zernike phase contrast mode with a spatial resolution of 50 nm, field of view of 16 µm x 16 µm and an illumination time of 200 s. The images were reference corrected.

Focused-ion beam (FIB) milling of MOF supraparticles.

A 3 µL droplet of oil containing the MOF supraparticles was casted onto a sticky carbon pad on the SEM stub. 20 nm carbon was deposited on top of the MOF supraparticles as a protection layer before inserting the sample into SEM/FIB. FIB cross sectioning of the particles and subsequent SEM imaging was performed on a Helios NanoLab 660 DualBeam SEM/FIB instrument. FIB milling was performed using Ga+ ions at 30 kV acceleration voltage and beam currents of 0.8 - 2.5 nA. Cross sectional imaging was performed using the backscattered electron signal at 1 - 2 kV acceleration voltage and 25 - 100 pA beam current in 38° inclined view with respect to the cross section with the image tilt correction being enabled.

Optical characterization of MOF supraparticles.

Microscopic reflection spectra of individual MOF supraparticle: A 3 µL droplet of oil containing the MOF supraparticles was casted onto clean glass substrate. After oil evaporation, isolated MOF supraparticles were successfully deposited on the substrate. Microscopic images were taken via a custom-modified (A.S. & Co.) Zeiss Axio Imager. Z2 in reflection mode using a Zeiss Epiplan 100x/NA0.75 and a CMOS camera (Zeiss Axiocam 208

color) with the field diaphragm partially closed and the aperture completely closed to the minimum opening. Spectra were measured by coupling light out via an optical fiber to a CCD spectrometer (Zeiss MCS CCD/UV-NIR). The outcoupling resulted in a measurement spot with an approximate diameter of 18 µm. Spectra were recorded by taking the average of 20 individual spectra integrated for around 150 µs; all with respect to a silver mirror as a 100% reflection reference.

Macroscopic reflection spectra of MOF supraparticles in suspension: For the angle-dependent reflection spectra measurements, a tungsten halogen light source (HL-2000-FSHA, ocean optics) was used for illumination. MOF supraparticles were suspended in 600 µL HFE 7500 oil in a 1.5 mL clear glass vial. The incident light was focused in an area (2mm in diameter) normal to the glass vial below the oil-air interface to illuminate the samples of MOF supraparticles in dispersion. The scattered light was collected using a collimator (2 mm spotsize) connected via class fibre to a Flame-T-VIS-NR-ES spectrometer (ocean optics). While the direction of the light source is fixed, both the sample and the collimator are mounted on a rotational stage. A clear glass vial containing the same amount of HFE 7500 oil without supraparticles was measured and used as a reference. Angle-dependent measurement was performed by rotating the stage from 30°, 45°, 60°, 75° to 90°. As the MOF supraparticles have lower density than the HFE 7500 oil, the samples constantly rise up to the oil-air interface. The vial is shaken to redistribute the samples homogeneously and inserted onto the stage immediately before each measurement. This dynamically changing concentration prevents the direct and quantitative comparison of the reflected light intensity.

Photograph of MOF supraparticles in suspension: Angle-depended photographs of MOF supraparitcle suspension in glass vials were taken using a Sony A6400 with a Laowa 65 mm f/2.8 2:1 Ultra Makro. The samples were illuminated by a photo flash (Godox V1), with a snoot (Godox AK-R1) attached. The illumination-angle was further restricted by a custom-made snoot-elongation.

Simulation of hard polyhedral particles in spherical confinement:

MOF particles were simulated with a Monte Carlo algorithm as hard polyhedra with excluded volume interactions. The four shapes are cube, truncated rhombic (truncation parameter *t*) dodecahedron, (perfect, i.e. $t = 0$) rhombic dodecahedron, and octahedron. Overlaps were checked with the Gilbert-Johnson-Keerthi algorithm.[4,5] Spherical confinement was realized by rejecting translations and rotations of polyhedra that moved one or more vertices outside of the confining sphere. Because the shapes studied here are convex, it is sufficient to test the vertices. 2000 hard polyhedra were placed in the spherical confinement. Simulations were set up at low density (10%) and then compressed up to target density (53%) for 10^7 Monte Carlo cycles. Snapshots were created using ambient occlusion shading in Injavis.[6]

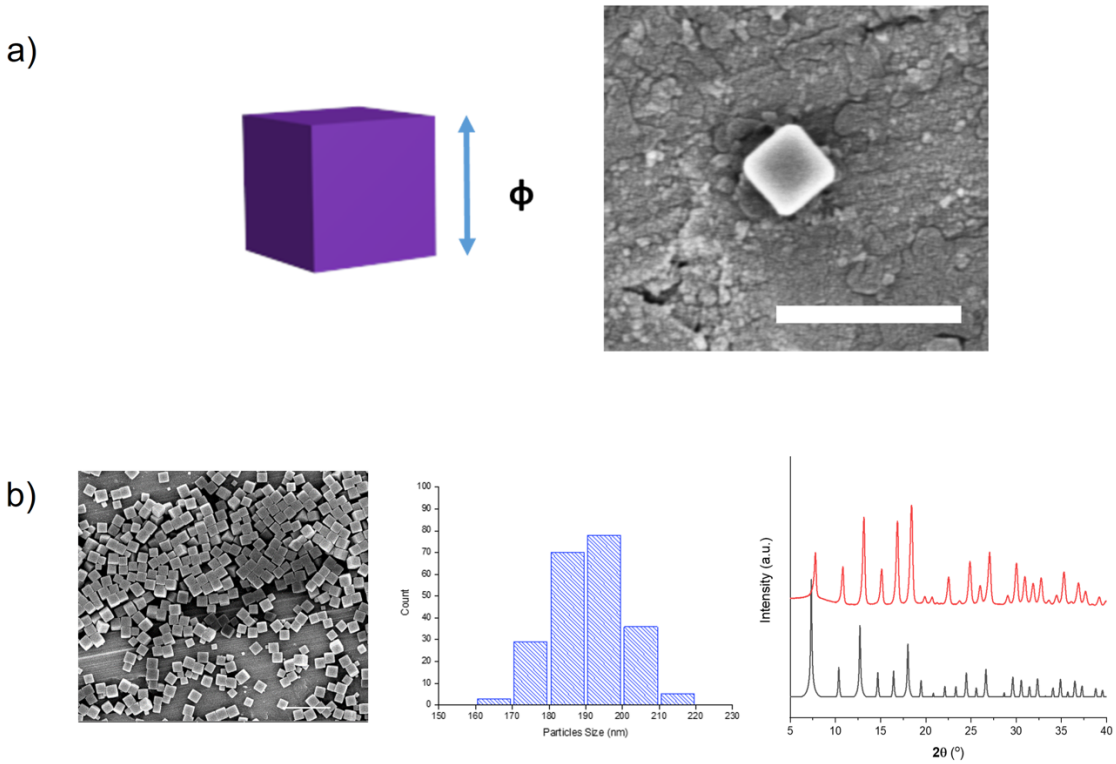

Figure S1. (a) Scheme and FESEM image of an as-synthesized C-ZIF-8 particle, highlighting the edge length (ϕ). Scale bar: 500 nm. (b) Left: Representative FE-SEM image of C-ZIF-8 particles. Scale bar: 1 μm. Middle: Size-distribution histogram of as-synthesized C-ZIF-8 particles with a mean ϕ of 191 ± 9 nm. Right: PXRD patterns of simulated (black) and as-synthesized C-ZIF-8 particles (red).

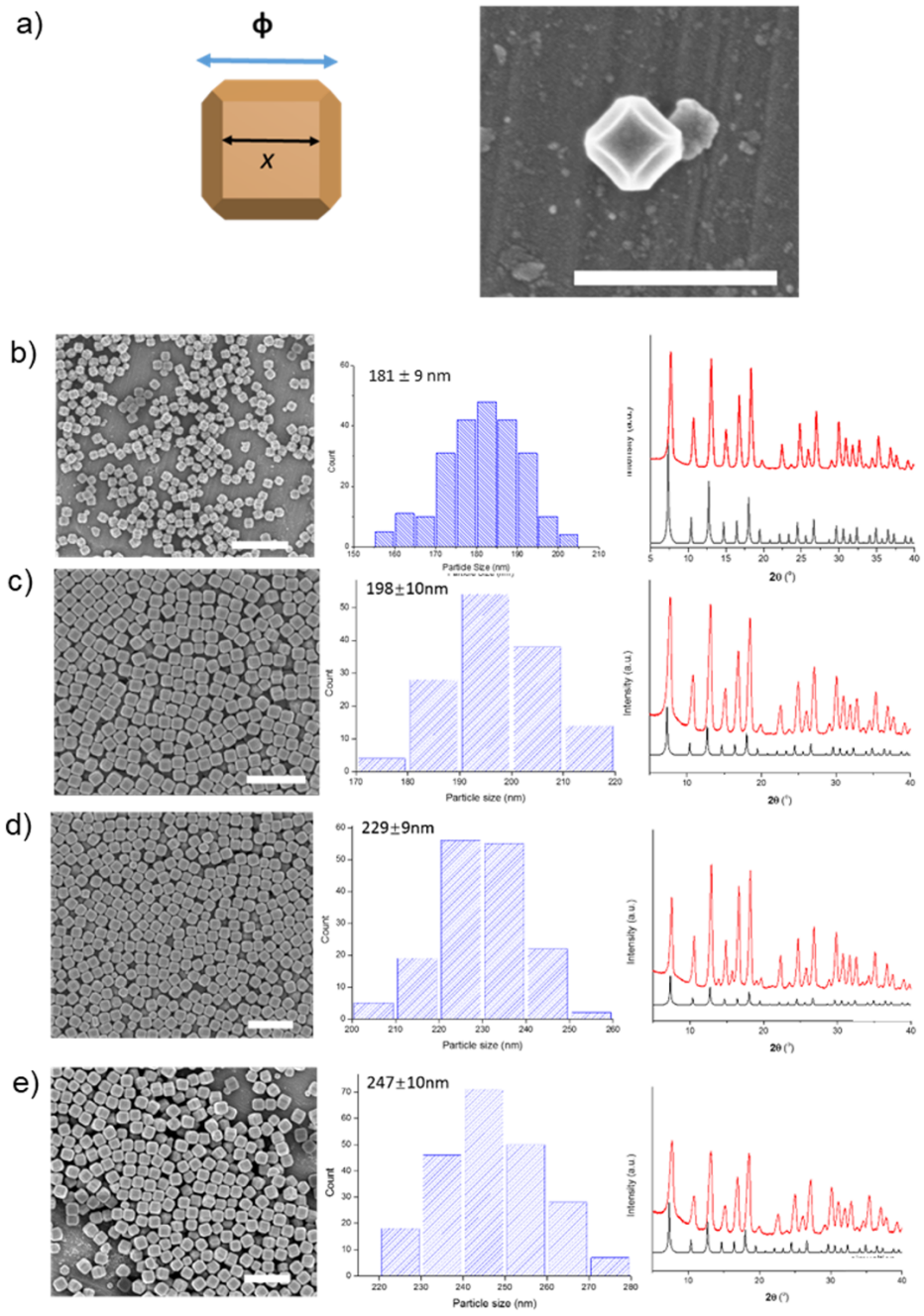

Figure S2. (a) Scheme and FESEM image of an as-synthesized TRD-ZIF-8 particle, highlighting the particle size (ϕ) and edge length (*x*). Scale bar: 500 nm. (b-e) TRD ZIF-8 particles (t= 0.68) with a mean ϕ of 181 ± 9 nm (b), 198 ± 10 nm (c), 229 ± 9 nm (d) and 247 ± 10 nm (e). Left: Representative FE-SEM images; Middle: Size-distribution histograms; and Right: PXRD patterns of simulated (black) and as-synthesized TRD-ZIF-8 particles (red).

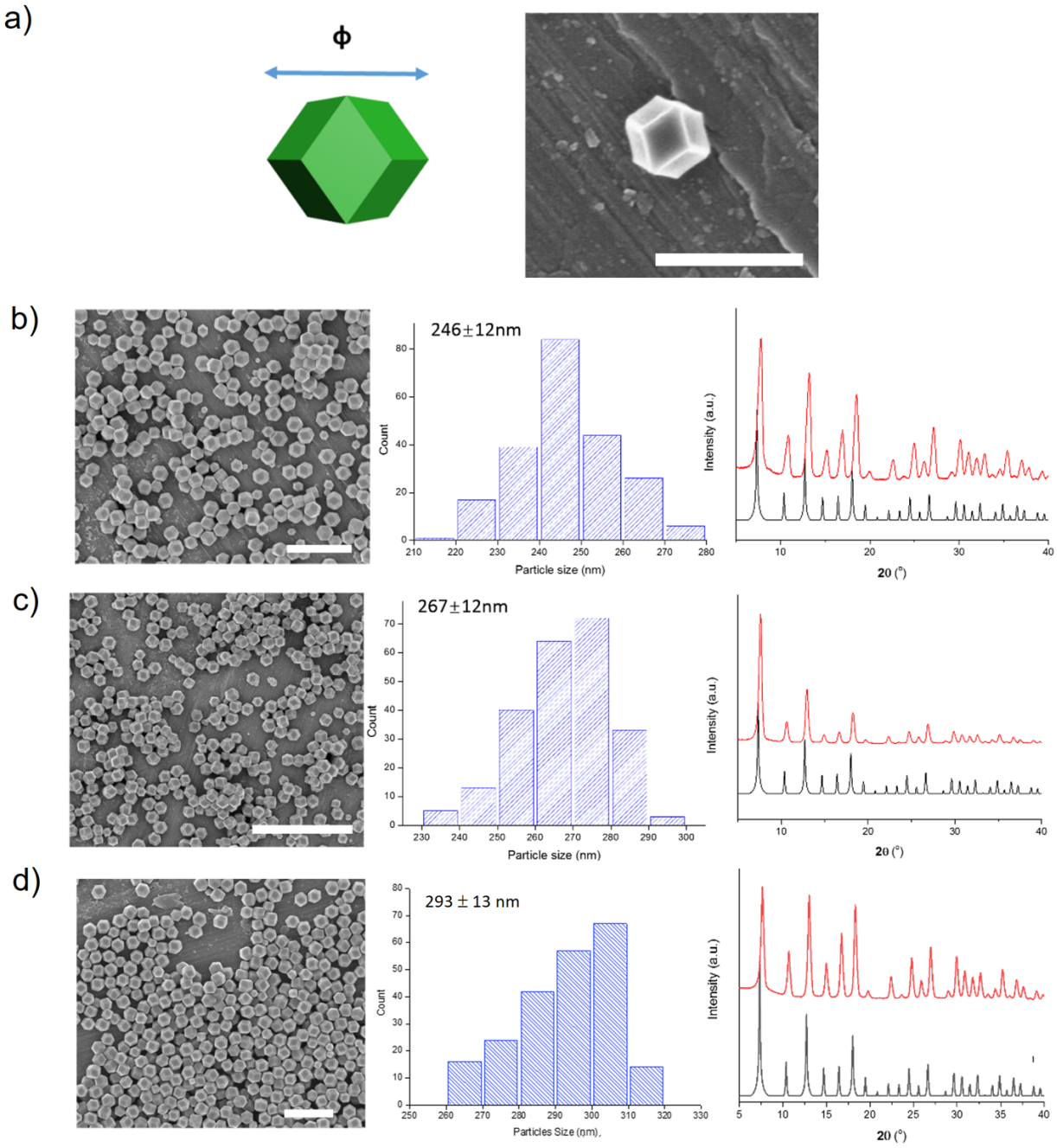

Figure S3. (a) Scheme and FESEM image of an as-synthesized RD-ZIF-8 particle, highlighting the particle size (ϕ). Scale bar: 500 nm. (b-e) RD ZIF-8 particles with a mean ϕ of 246 ± 12 nm (b), 267 ± 12 nm (c), and 293 ± 13 nm (d). Left: Representative FE-SEM images; Middle: Size-distribution histograms; and Right: PXRD patterns of simulated (black) and as-synthesized RD-ZIF-8 particles (red).

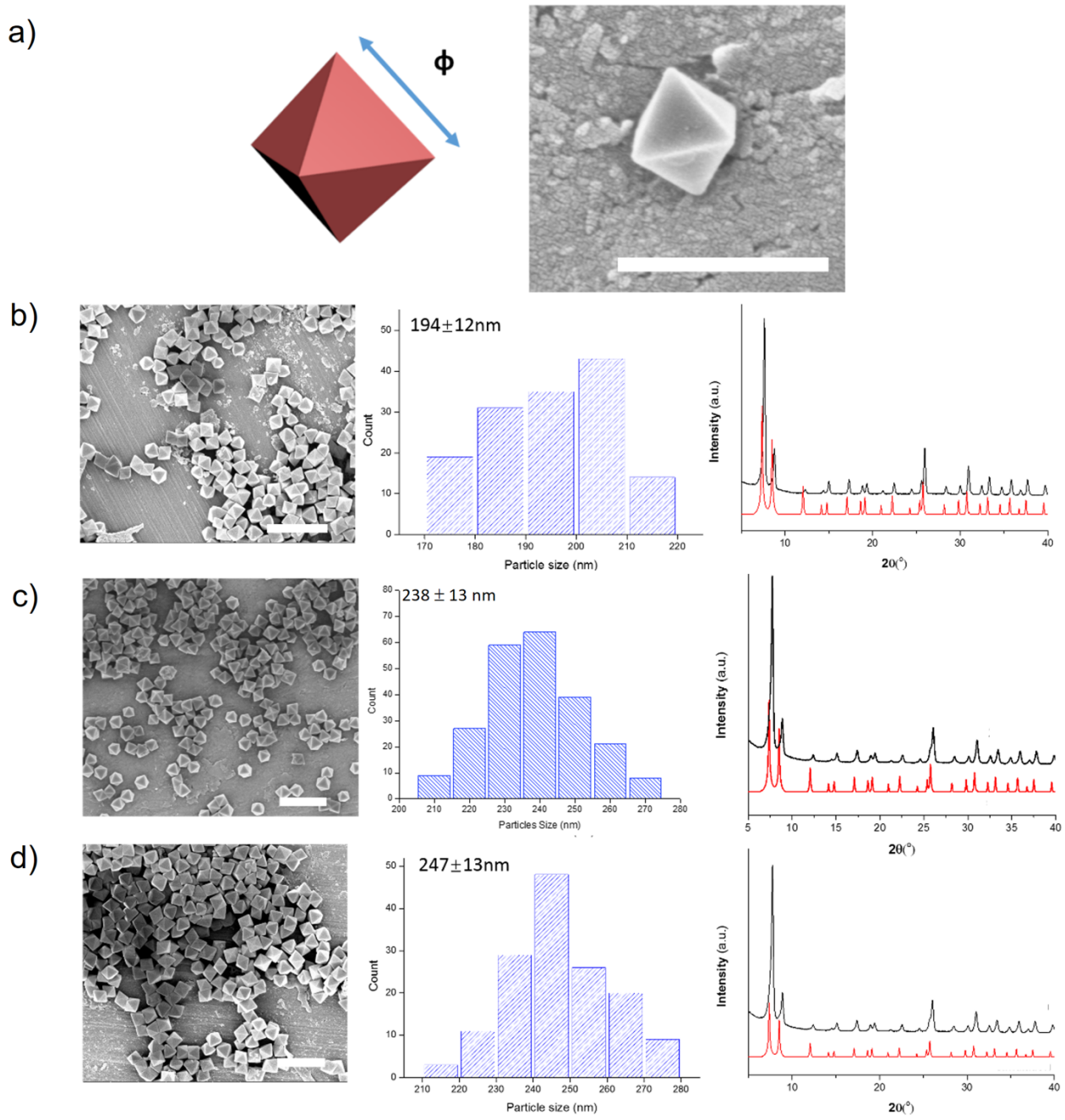

Figure S4. (a) Scheme and FESEM image of an as-synthesized O-UiO-66 particle, highlighting the edge length of particles (ϕ). Scale bar: 500 nm. O-UiO-66 particles a mean ϕ of 194 ± 12 nm (b), 238 ± 13 nm (c), and 247 ± 13 nm (d). Left: Representative FE-SEM images; Middle: Size-distribution histograms; and Right: PXRD patterns of simulated (black) and as-synthesized RD-ZIF-8 particles (red).

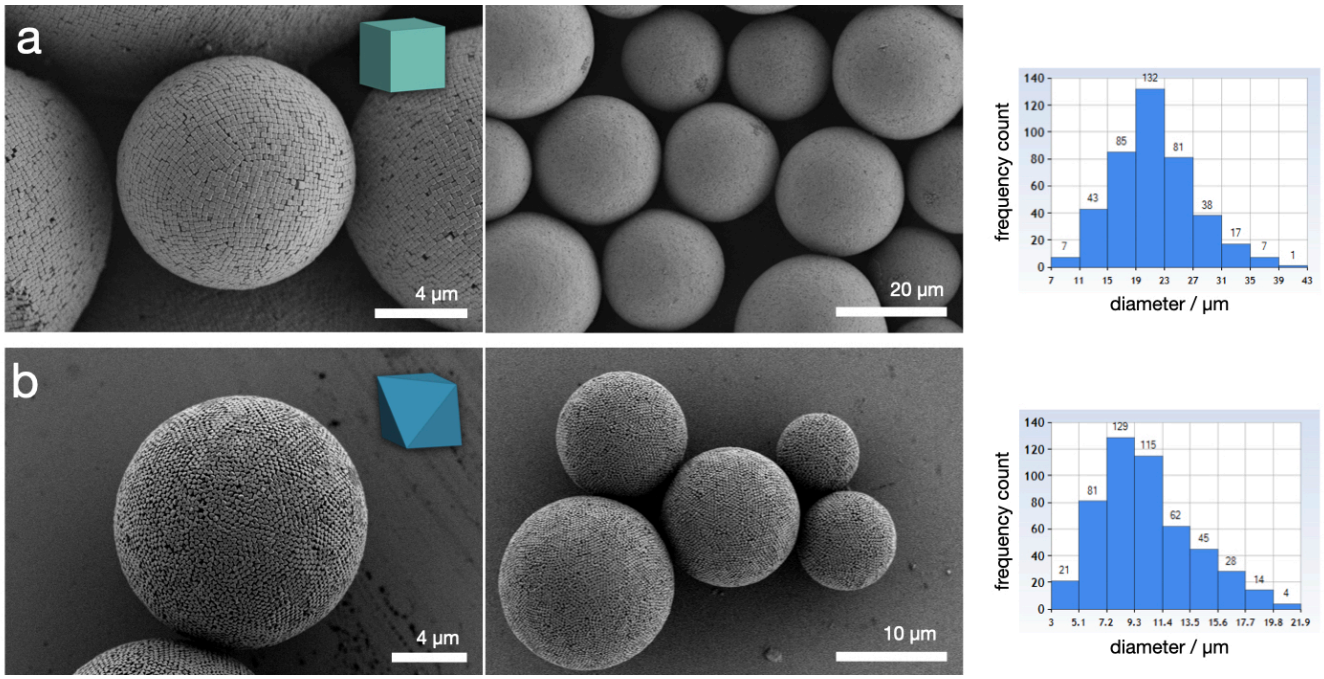

Figure S5. Representative FESEM images of polydisperse C-ZIF-8 (a) and O-UiO-66 (b) supraparticles prepared by shaking emulsifying, with a size of 21 ± 5.6 µm (26% polydispersity) and 9.9 ± 3.4 µm (34% polydispersity, approximately 500 counts), respectively. The dimensions of the produced supraparticles depends on the time duration and power input of the emulsification. Details of emulsification is described in the Experimental Procedure section.

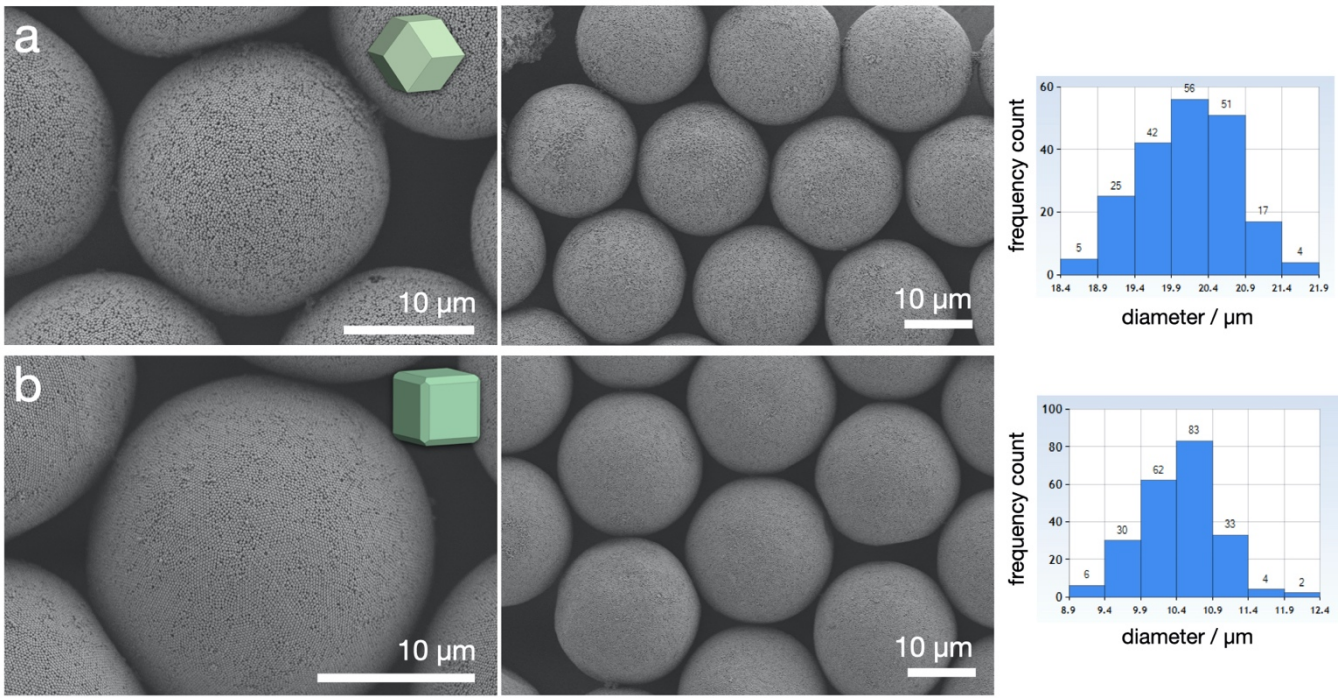

Figure S6. Representative FESEM images of monodispersed RD-ZIF-8 (**a**) and TRD-ZIF-8 (**b**) supraparticles prepared using a droplet-based microfluidic device, with a size of 20.1 ± 0.6 μm (3% polydispersity) and 10.4 ± 0.5 μm (5% polydispersity, approximately 200 counts), respectively. The size can be controlled by varying flow rates in the microfluidic device. Details of the emulsification is described in Experimental Procedure section.

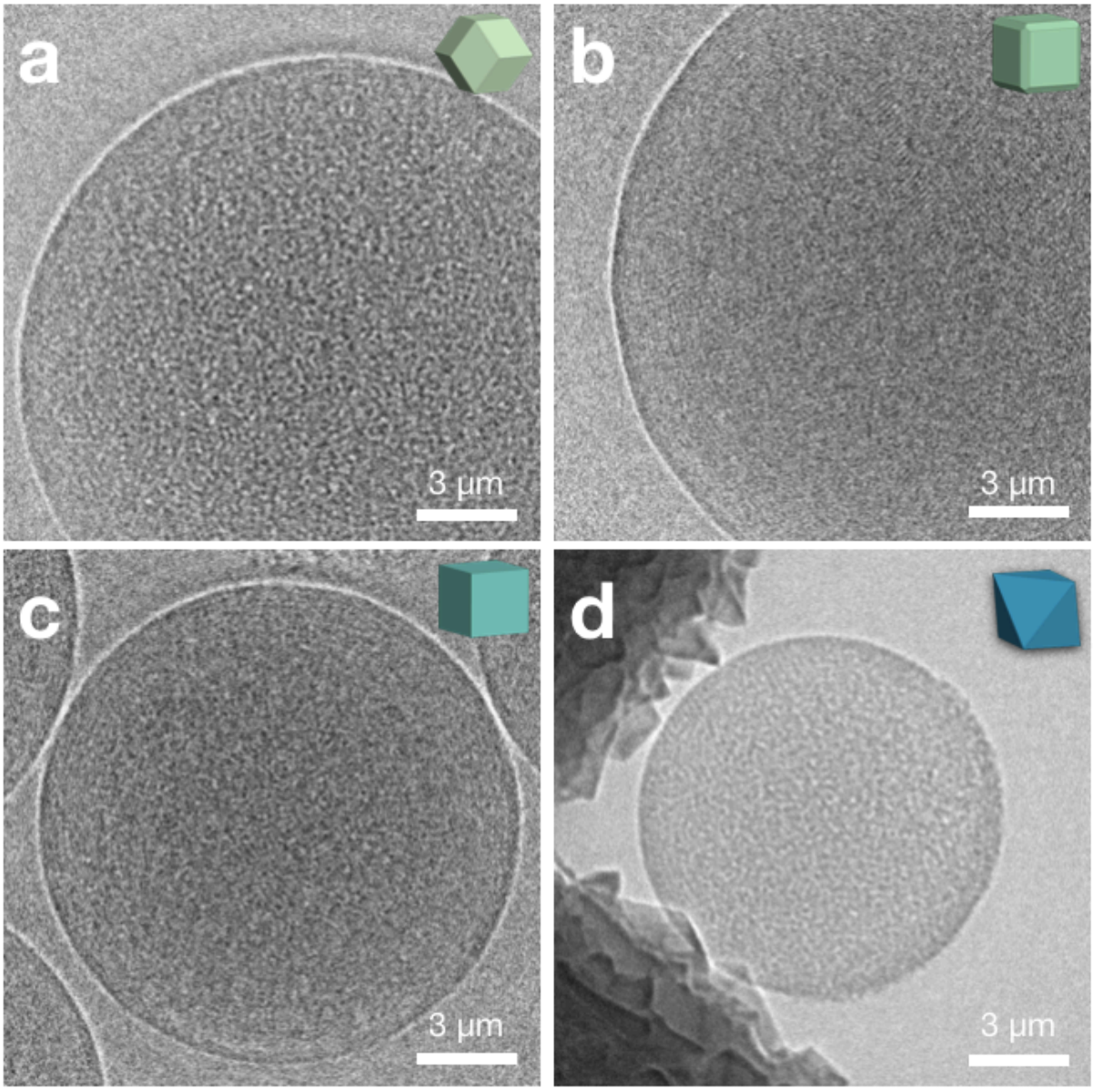

Figure S7. Transmissive X-ray image of MOF supraparticles of a) RD-ZIF-8, showing few onion-like layers near the surface; b) TRD-ZIF-8, showing thick onion-like layers, as well as some lattice fringes; c) C-ZIF-8, showing thick onion-like layers, as well as some lattice fringes; and d) O-UiO-66 particles, showing only little onion-like layer structures.

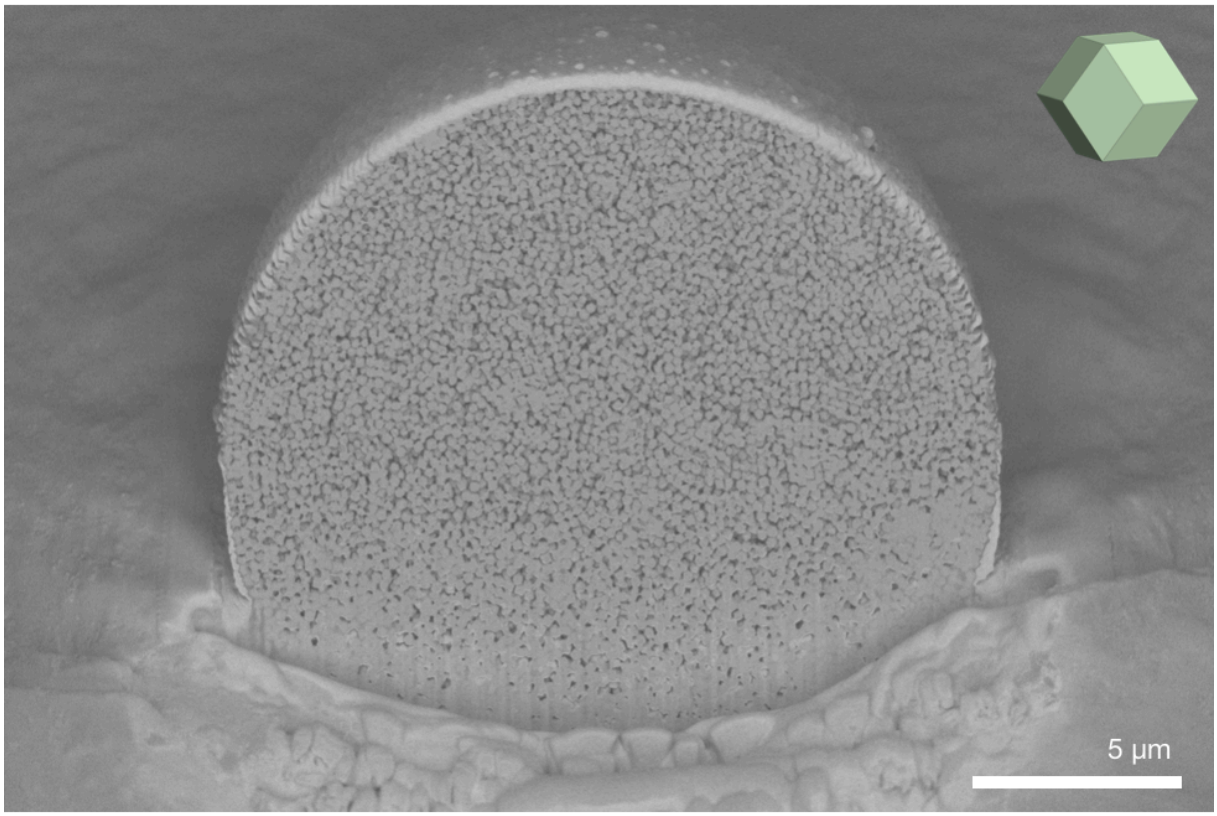

Figure S8. Cross-section of RD-ZIF-8 supraparticles revealed by focused-ion beam milling.

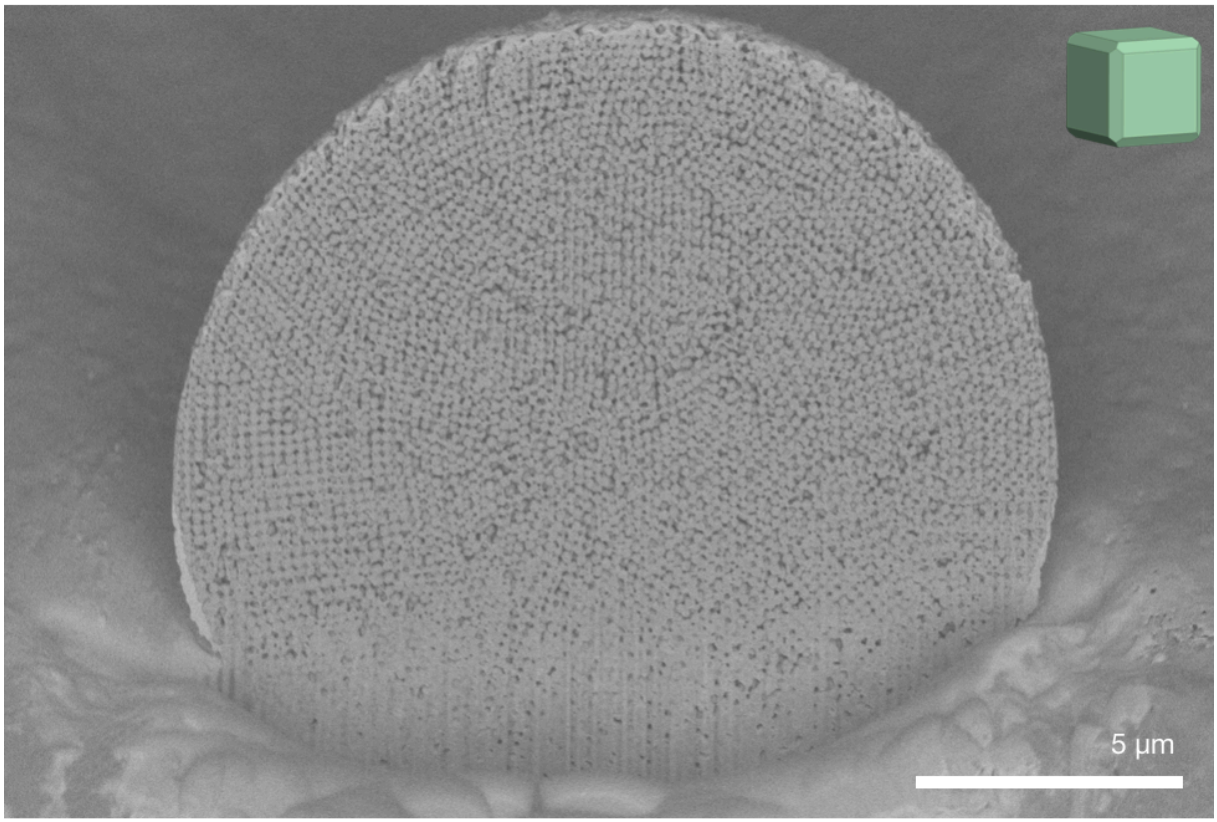

Figure S9. Cross-section of TRD-ZIF-8 supraparticles revealed by focused-ion beam milling.

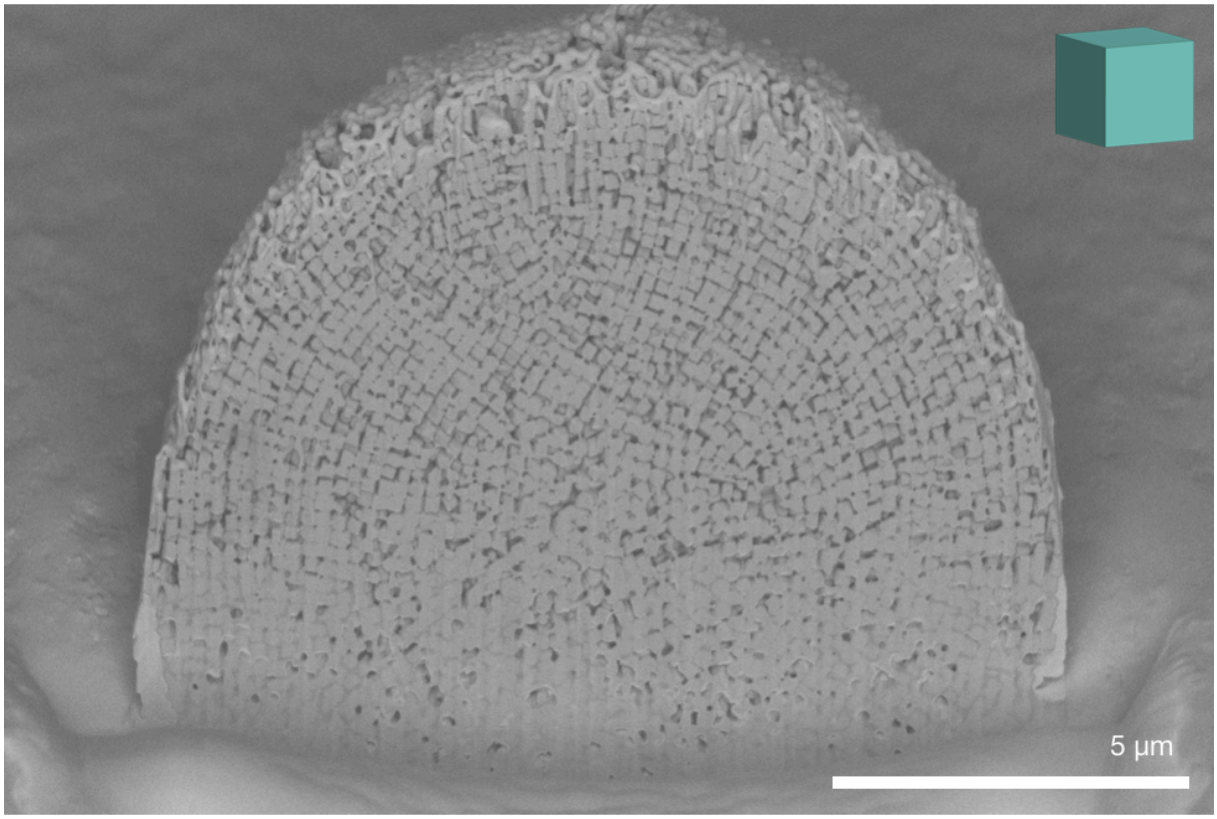

Figure S10. Cross-section of C-ZIF-8 supraparticles revealed by focused-ion beam milling.

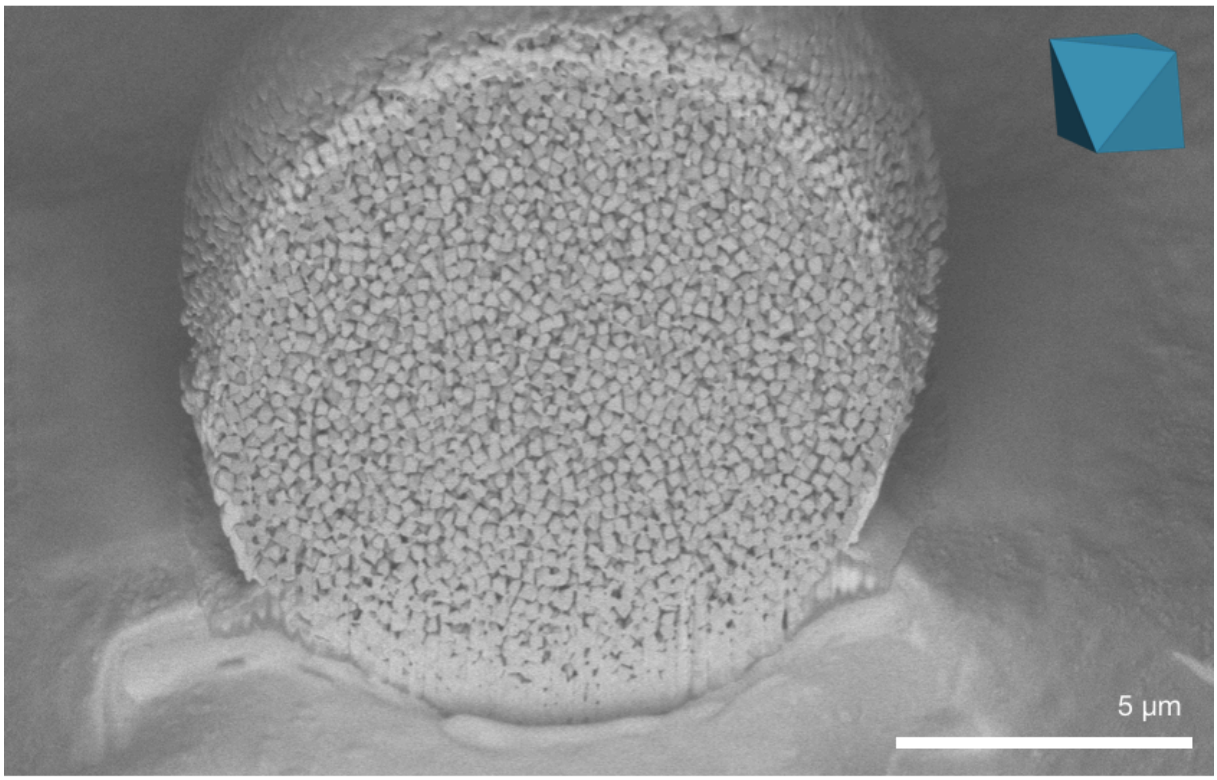

Figure S11. Cross-section of O-UiO-66 supraparticles revealed by focused-ion beam milling.

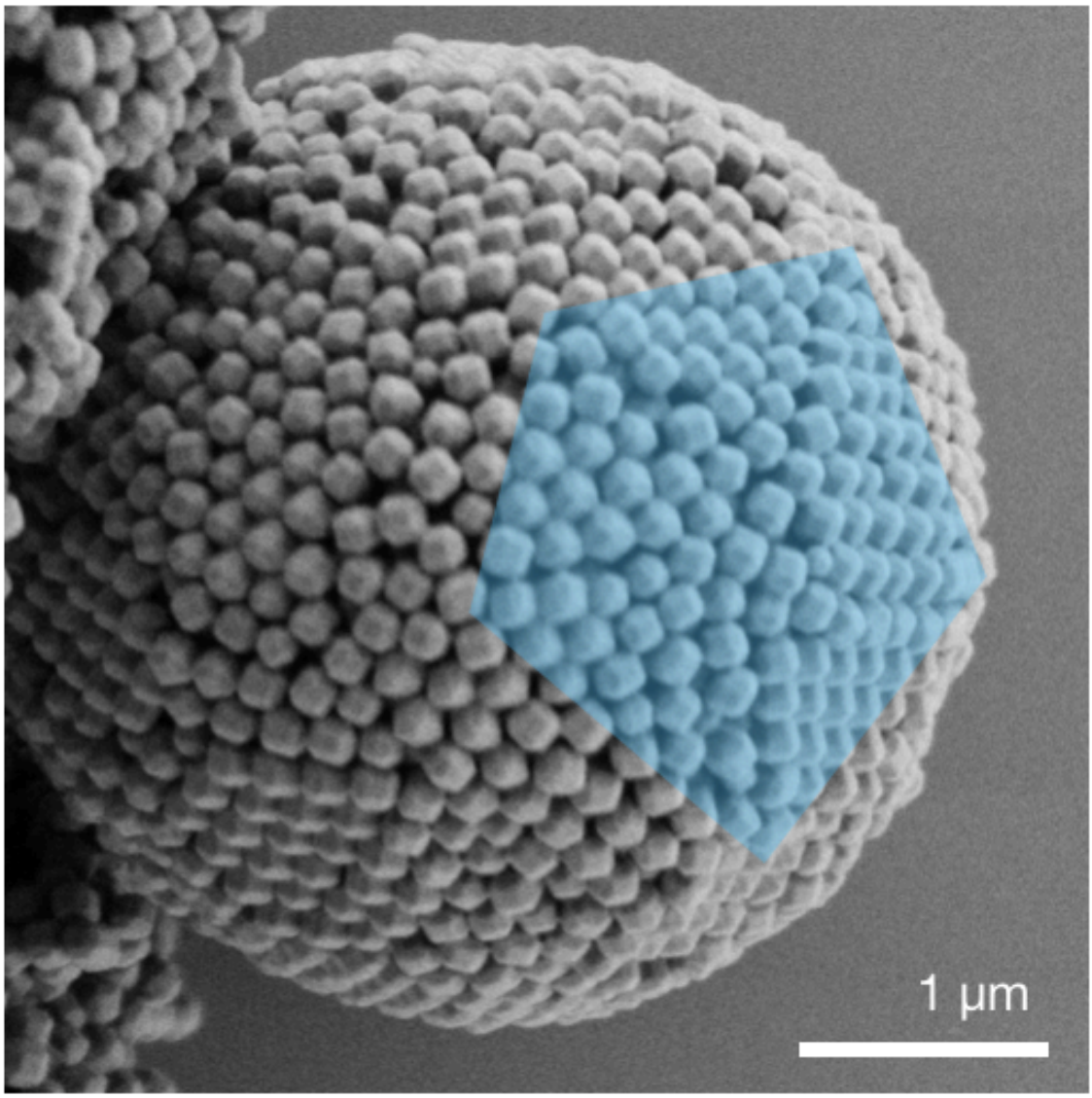

Figure S12. A TRD-ZIF-8 supraparticle exhibiting local five-fold symmetric surface pattern, marked with blue colour.

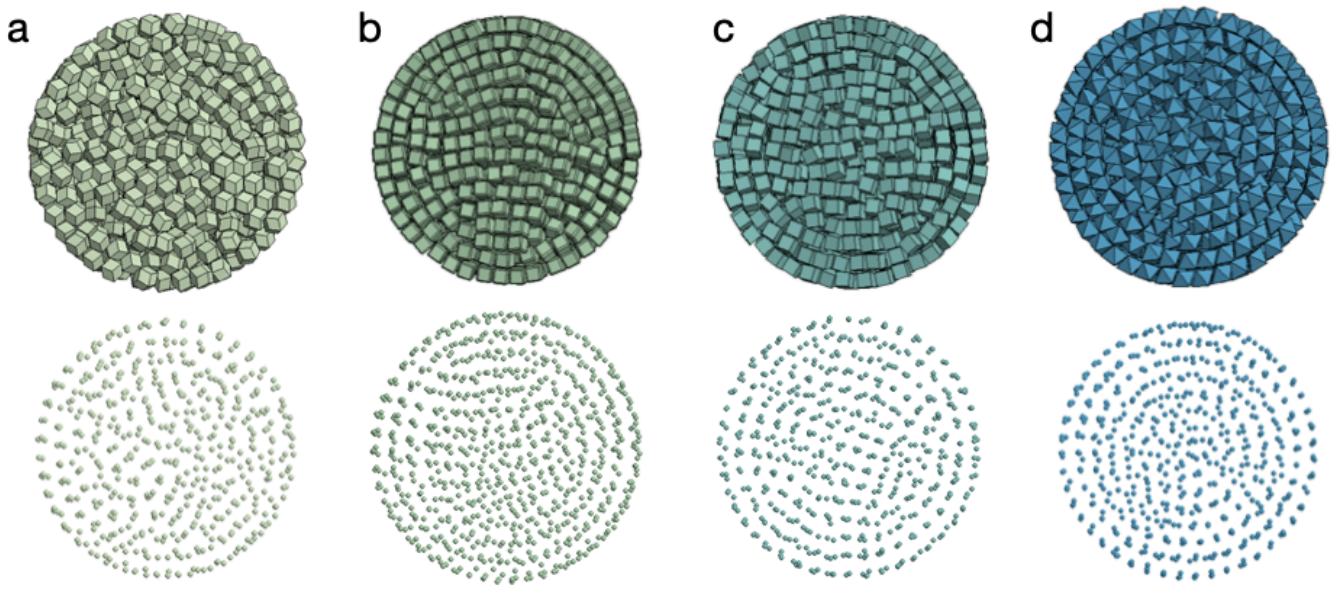

Figure S13. Cross-sectional images of simulated supraparticles of hard polyhedra in spherical confinement. All shapes (rhombic dodecahedron (**a**), truncated rhombic dodecahedron (**b**), cube (**c**), octahedron (**d**)) form three to four onion-like layers near the confinement surface (upper row: rendering of particle at the cross-section, lower row: particles in the cross-sectional regions, each dot represents the geometric center of a particle). Cube particles form body-center cubic lattice in the interior. Octahedron particles form the thickest onion layers. The contrast to experimental observation suggests that the MOF particles in droplets in our experiments cannot be approximated as hard polyhedral-like particles.

Figure S14. Photograph of the self-assembled superstructures resulting from the centrifugation of different aqueous colloidal MOF particles (from left to right: RD-ZIF-8, TRD-ZIF-8, C-ZIF-8 and O-UiO-66). Strong iridescence is observed for TRD-ZIF-8 sample. Weak iridescence is observed for C-ZIF-8 sample. No color is observed for RD-ZIF-8 and O-UiO-66 samples.

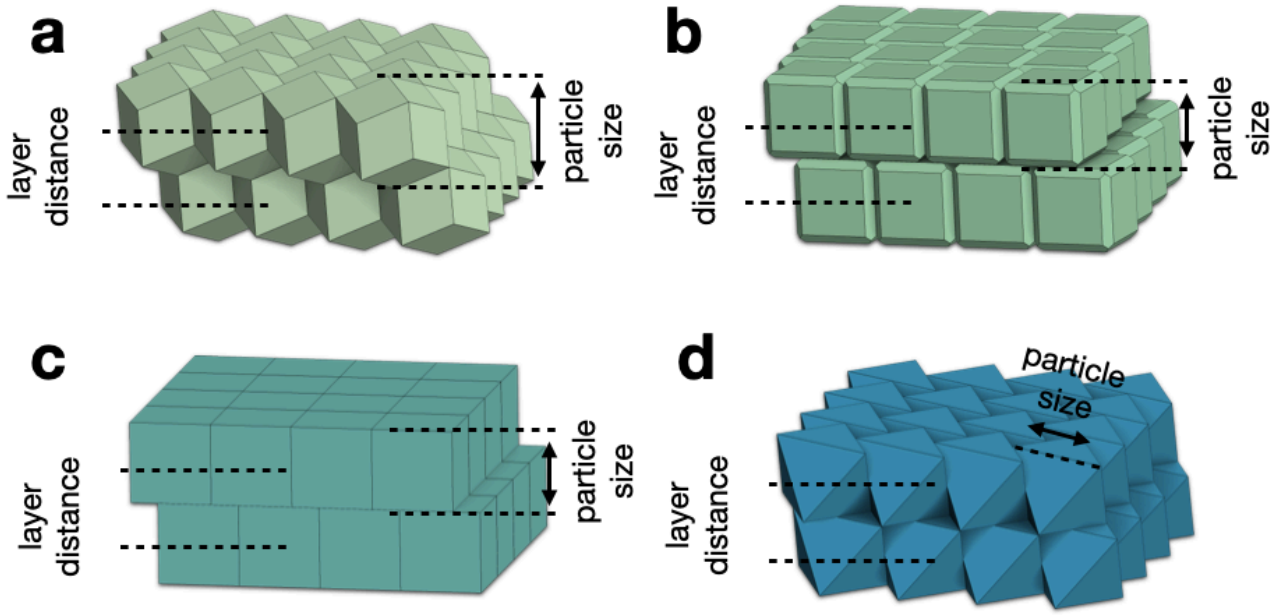

Figure S15. Relationship between MOF particle size of different shapes and layer distance. For RD-ZIF-8 particles, the protrusion and indentation on the surface of the close-packed layer can register with neighboring layer and bring them closer than the size of the particle (**a**). For TRD- and C-ZIF-8 particles, the close-packed layer has a "flat" surface, the layer distance equals to the particle size (**b**,**c**). For O-UiO-66 particles, the layer distance equals to the distance between two parallel faces of the octahedron, which is approximately 0.8 of the particle size (edge length of octahedron, **d**). The definition of sizes for polyhedral MOF particles follows the tradition to provide reference in the MOF community. It is in general difficult to have a simple yet consistent definition. Measuring TRD-ZIF-8 edge length results in large deviation due to the small truncation in the SEM image, the farthest vertex distance (used in RD-ZIF-8) is difficult to measure for O-UiO-66 particles.

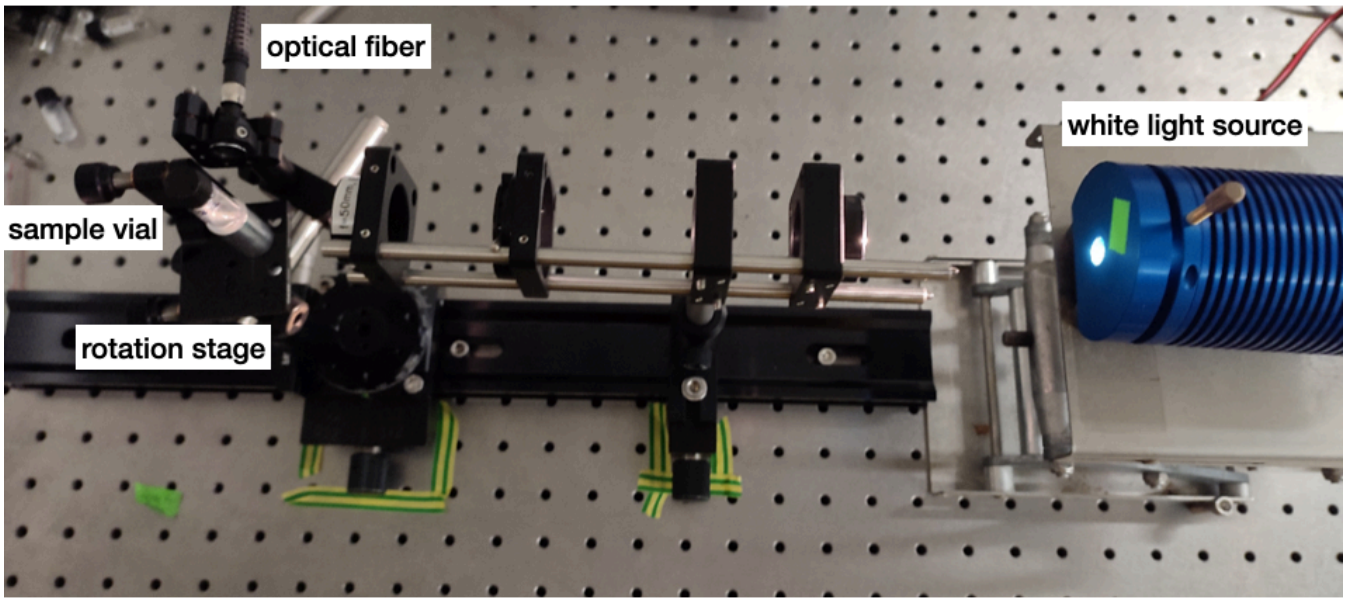

Figure S16. Optical setup to measure reflectance spectra directly from MOF supraparticles suspended in liquid in a glass vial. This enables the angle-dependent optical characterization of a large number of supraparticles at once, and directly in dispersion.

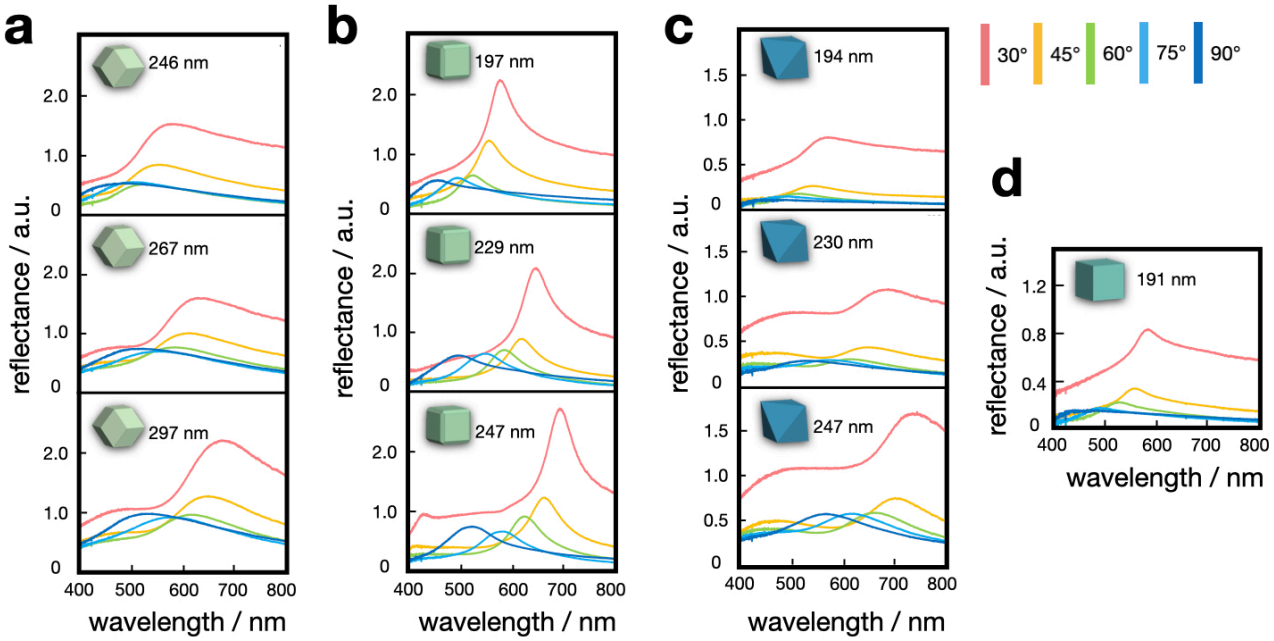

Figure S17. Angle-dependent reflection spectra of four types of MOF supraparticles measured directly from liquid suspension. For all samples, the reflection peaks move towards larger wavelengths with increasing particle sizes, and towards lower wavelength with larger angles between incident light and observation.

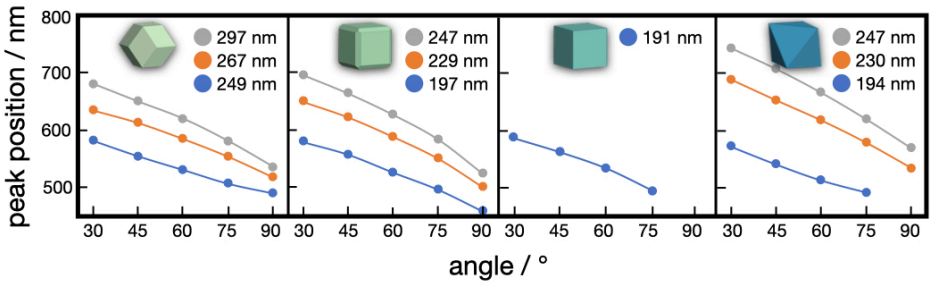

Figure S18. Shift of the reflectance peak with increasing viewing angle for four types of MOF supraparticles. Particle size, shape and material type do not show a discernable influence on the peak shift.

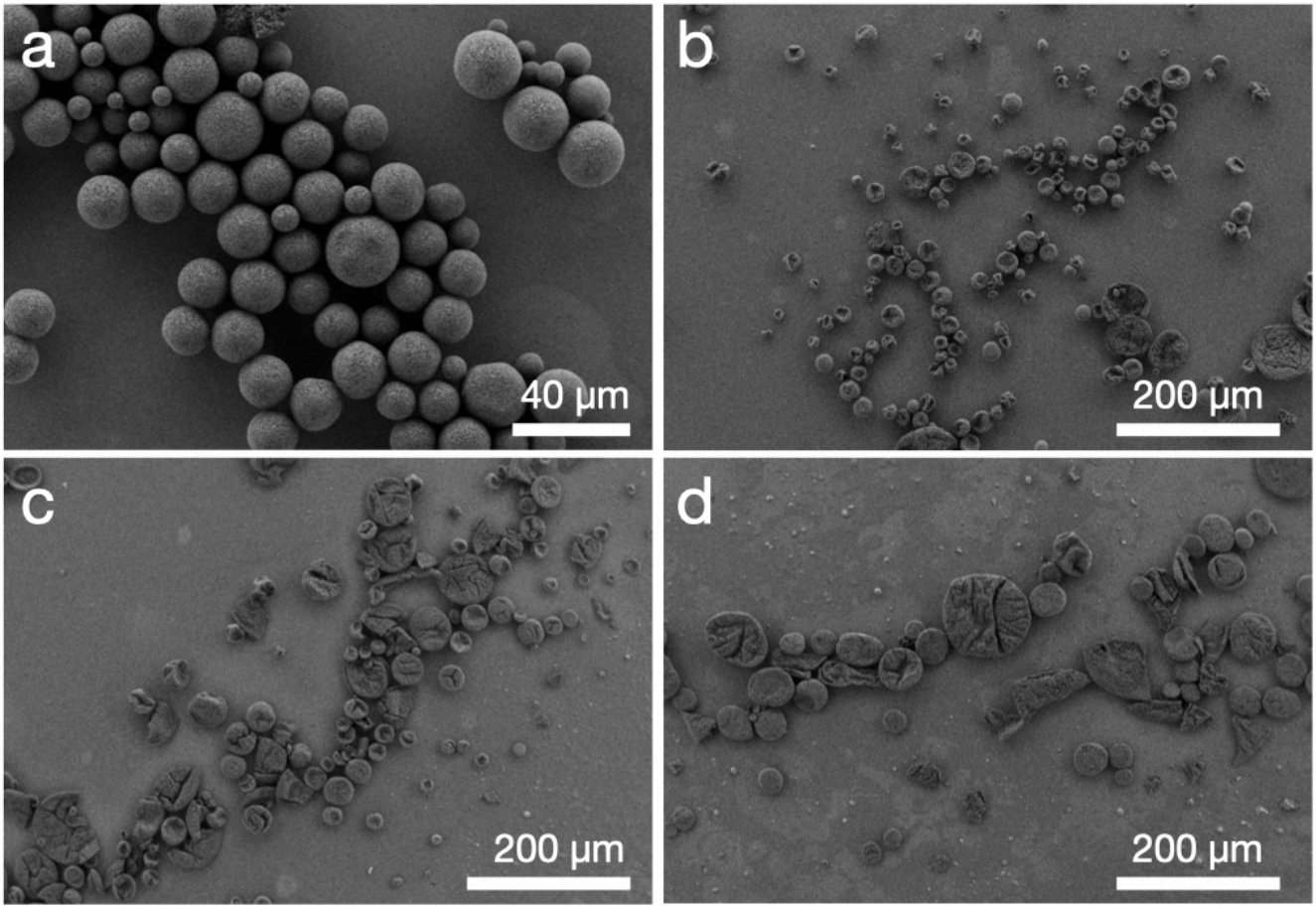

Figure S19. Buckled RD-ZIF-8 supraparticles. 1.0 mL 1 wt% Lutensol TO8 surfactant is added to 0.5 mL 2 wt% RD-ZIF-8 particle dispersion. The dispersion is centrifuged four times. After each centrifuge circle, 10 µL of particle dispersion is emulsified in 200 µL of HFE 7500 oil containing 1 wt% perfluorinated surfactant for subsequent drying into MOF supraparticles. Spherical supraparticles are formed after one centrifuge cycle (a), buckled supraparticles are formed after two, three and four centrifuge cycles (b,c,d). We note that influence of surfactant on the self-assembly of MOF particles in droplet is complex. For a combination of 0.5 mL 1 wt% Lutensol TO8 and 1.0 mL 2 wt% RD-ZIF-8 (synthesized in the same batch), all four centrifuge cycles resulted in spherical supraparitcles. The tendency to buckle also depends on the shape of particles, TRD-ZIF-8 particles formed spherical supraparticles even without the addition of surfactant.

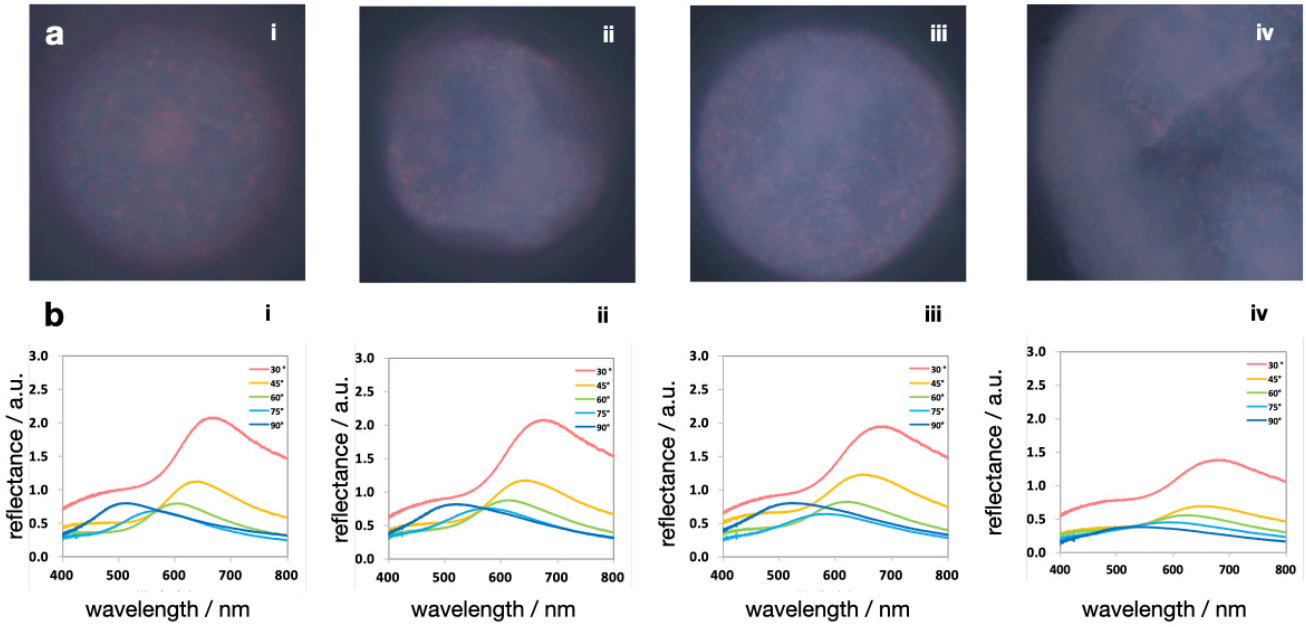

Figure S20. Angle-dependent reflection spectra of buckled MOF supraparticles measured directly from suspension. Supraparticles with increasing deviations from spherical geometry and more buckling are produced from RD-ZIF-8 MOF primary particles (**a**, from i to iv) by increasing centrifugation cycles to remove the surfactant. Note that all samples exhibit macroscopic, angle-dependent structural color (bottom row) even though the observable microscopic coloration at the single particle level is reduced (top row).

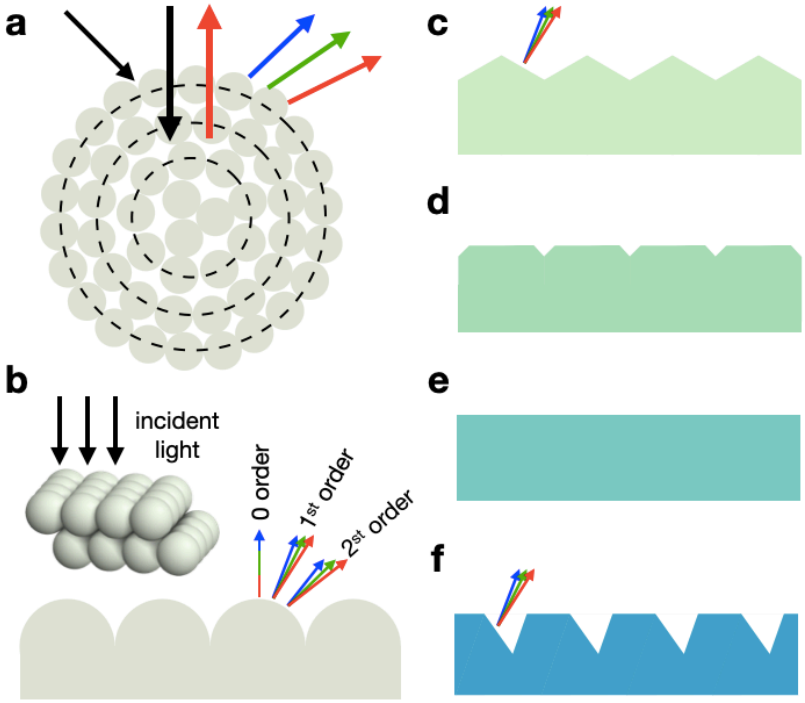

Figure S21. Hypothesized surface grating effects of MOF supraparticles. Typical spherical supraparticles consisting of spherical particles form concentric onion-like layers (**a**), which creates alternating refractive index that produces color by Bragg reflection at the onion-like layers. In addition, parts of the incident light are also diffracted from the supraparticle surface, where the ordered particles form a nanostructured surface grating. Layers consisting of spherical particles resembles a grating with sinusoidal groove, which disperse light into several diffraction orders at different angles (**b**). Polyhedral particles can create surfaces with sharp protrusion of large inclination angles, which resembles a blazed grating (**c** for RD-ZIF-8, **d** for TRD-ZIF-8, **f** for O-UiO-66 particles). The blazed grating is known to have higher diffraction efficiency at non-zero diffraction order. Cubic shape creates surfaces with little to no grooves (**e** for C-ZIF-8 particles).

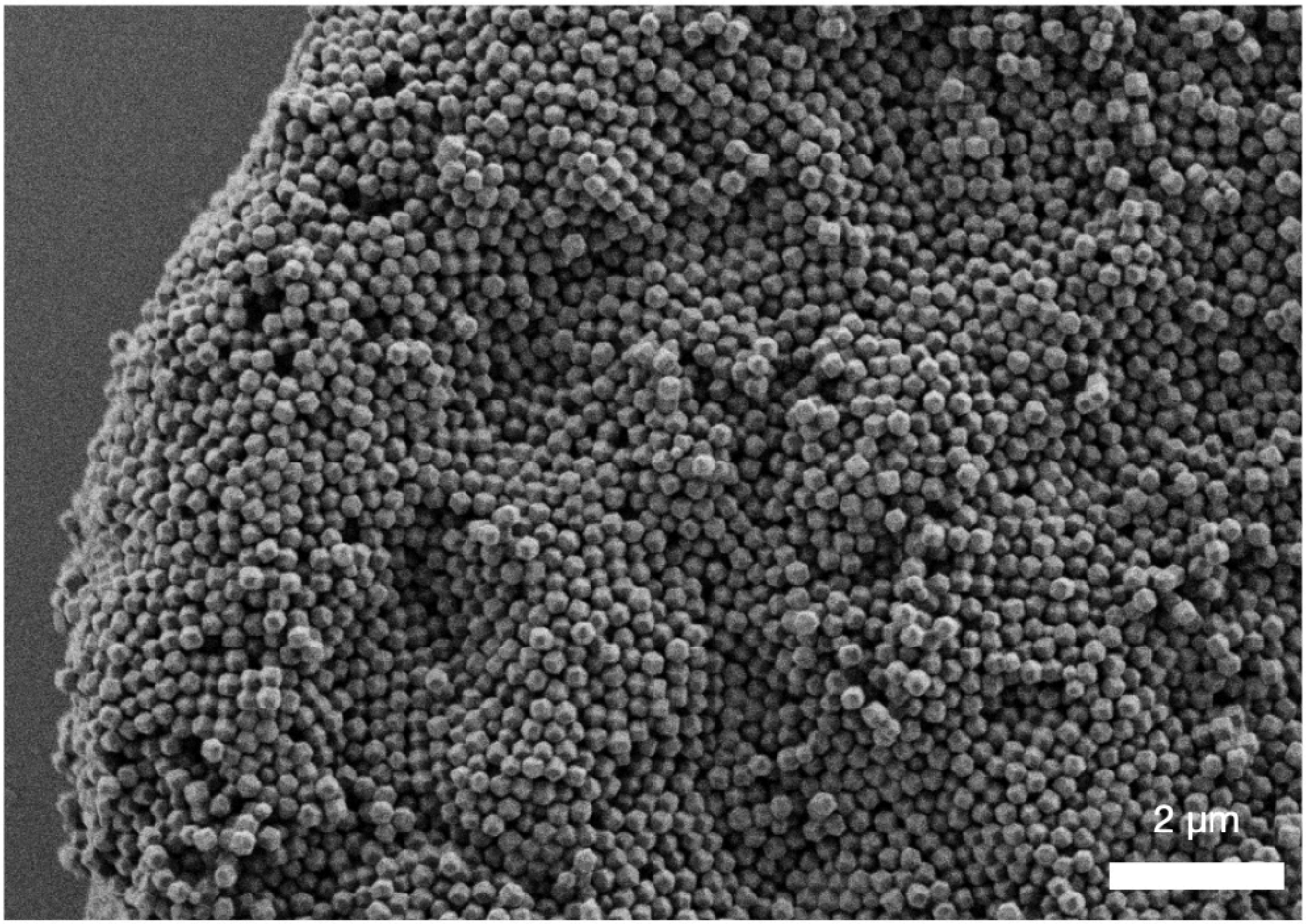

Figure S22. Buckled RD-ZIF-8 supraparticles exhibit ordered surface features, visualized in scanning electron microscopy.

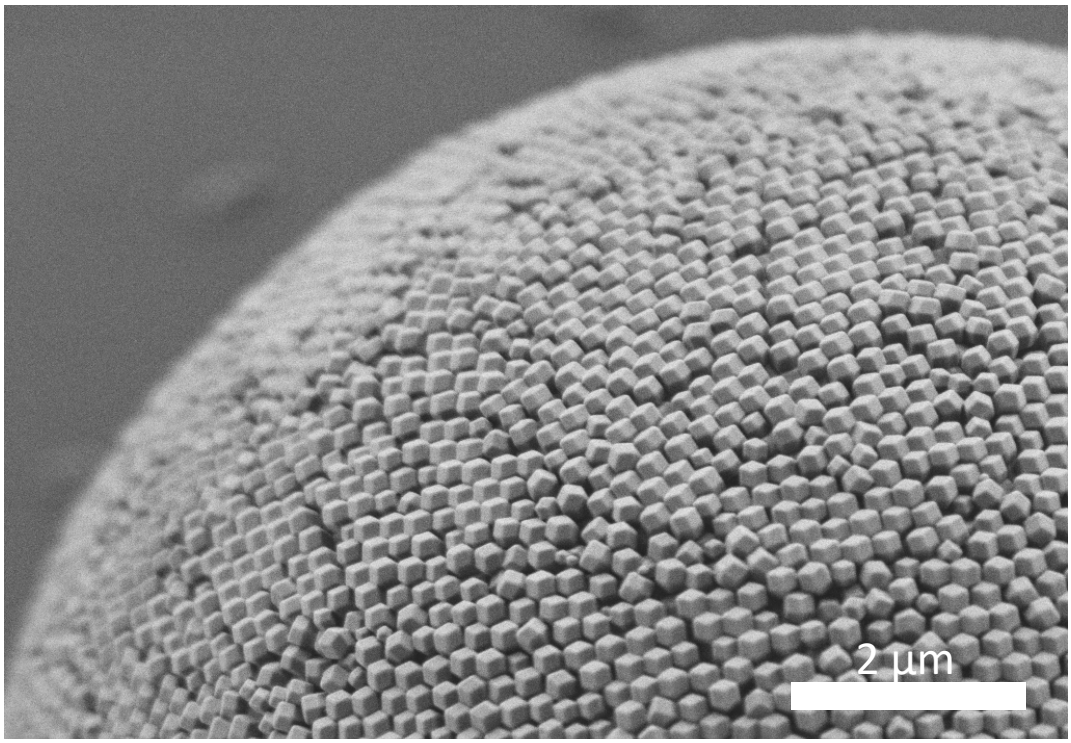

Figure S23. The surface packing of RD ZIF-8 supraparticles shows a sawtooth groove profile, as seen in scanning electron microscopy

References

[1] C. Avci, I. Imaz, A. Carné-Sánchez, J. A. Pariente, N. Tasios, J. Pérez-Carvajal, M. I. Alonso, A. Blanco, M. Dijkstra, C. López, D. Maspoch, *Nat. Chem.* **2018**, *10*, 78.

[2] R. Scanga, L. Chrastecka, R. Mohammad, A. Meadows, P.L. Quan, E. Brouzes, *RSC Adv*, **2018**, *8*, 12960.

[3] R. Birte, PhD thesis. Georg-August-Universität Göttingen (Germany), **2015.**

[4] E.G. Gilbert, D.W. Johnson, S.S. Keerthi, *IEEE J Robot Autom.* **1988**; *4*, 193- 203.

[5] P. F. Damasceno, M. Engel, S. C. Glotzer, *ACS Nano* **2012**, *6*, 609.

[6] M. Engel; 2021; INJAVIS - INteractive JAva VISualization; doi: 10.5281/zenodo.4639570.